

Study of a pair of coupled continuum equations modeling surface growth

A in-ul H udaz

S N . Bose National Centre for Basic Sciences, JD Block, Sector III, Salt Lake City,
Kolkata 700098, India

Om j yoti D uttax

Department of Electronics and Telecommunications, Jadavpur University, Kolkata
700032, India

A bhijit M ookerjee

S N . Bose National Centre for Basic Sciences, JD Block, Sector III, Salt Lake City,
Kolkata 700098, India

Abstract. In this communication we introduce a pair of coupled continuum equations to model overlayer growth with evaporation-accretion due to thermal or mechanical agitations of the substrate. We gain insight into the dynamics of growth via one-loop perturbative techniques. This allows us to analyze our numerical data. We conclude that there is a crossover behaviour from a roughening regime to a very long-time, large length scale smoothening regime.

PACS numbers: 71.20, 71.20c

1. Introduction

The dynamics of surface growth by atomic deposition have been the focus of interest over recent years ([1]–[8]). Several theoretical attempts ([9]) at the understanding of kinetic roughening have been made, through discrete and continuum models, motivated by experiments. Roughening is often an inevitable part of surface formation, so that an understanding of the surface morphologies has a crucial part to play in the many vital applications of this field. However, not much attention has been paid to the phenomenon

z email : huda@bose.res.in

x email : om_jyoti@redimail.com

k email : abhijit@bose.res.in

of smoothening by thermal effects like evaporation. The physical picture is clear : the vibration of the substrate, of thermal or mechanical origin may smoothen the overlayer surface by transferring weakly bonded atoms on its bumps or mounds to available surface grooves. The picture is similar, but certainly not equivalent, to smoothening of granular surfaces by avalanches. This is in contrast to the surface diffusion term in continuum models, which arises because of the internal rearrangement of the bonded atoms in order to minimize the chemical potential. Avalanche smoothening has been recently studied in some detail using coupled continuum equations by Biswas et al ([10]).

The notion that we shall borrow and adapt from the work of Biswas et al is that the dynamics of atoms in surface growth with evaporation-accretion is well described by the competition between the collective dynamics or relaxation of bonded atoms (in order to minimize the chemical potential) and the dynamics of free atoms diffusing on the surface. The bare surface of bonded, and therefore relatively immobile atoms, will be described by the local height $h(\underline{r};t)$ above the substrate. Across this surface the gas of unbonded evaporated atoms diffuse until they are captured in an available groove. This gas of atoms will be characterized by its density $\rho(\underline{r};t)$ just above the bare surface. A similar model has been discussed by Sanyal et al [11]. However, the transfer term in the equations was rather different from ours and the possibility of smoothening was not addressed in that work.

The usual practice for probing temporal or spatial roughness is to study the asymptotic behaviour of correlation functions like $\langle h(\underline{r};t)h(\underline{r}^0;t^0) \rangle$ in space or time via a single Fourier transform. Only one of the variables : space or time, is integrated over in Fourier space and the relevant scaling relations are used to determine the critical exponents that govern this behaviour. However, as pointed out by Biswas et al ([10]), this leads to ambiguities for those problems where there may be more than one scaling lengths. In such cases, the double Fourier transform provides a much deeper insight. To clarify this point, let us introduce the salient features of such a study :

The connected two point self-correlation function of the local variable $A(\underline{r};t)$, which can either be $h(\underline{r};t)$ or $\rho(\underline{r};t)$ is defined as :

$$S(\underline{r} - \underline{r}^0; t - t^0) = \langle A(\underline{r};t)A(\underline{r}^0;t^0) \rangle - \langle A(\underline{r};t) \rangle \langle A(\underline{r}^0;t^0) \rangle \quad (1)$$

The scaling hypothesis implies that we have, in the absence of spatial anisotropy,

$$S(\underline{R};0) \sim \underline{R}^{-\beta} \quad \underline{R} = \underline{r} - \underline{r}^0; \quad R = |\underline{R}| \quad \text{and} \quad R \gg 1$$

for the saturated surface with $t > t_s$, where t_s is the saturation time, and

$$S(0; \tau) \sim \tau^{-\beta} = \tau^{-\beta} \quad \tau \gg 1$$

In general,

$$S(\underline{R}; \tau) \sim R^{-\beta} \tau^{-\beta} \quad \text{for both } R, \tau \gg 1$$

The scaling function ϕ is universal, α is the roughness and $z = \alpha - \beta$ the dynamical exponent. For the single Fourier transform S ,

$$S(k; \omega = 0) \sim k^{-(1-\alpha)} \quad \text{for } k \neq 0$$

and

$$S(k = 0; \omega) \sim \omega^{-(1-\beta)} \quad \text{for } \omega \neq 0 \quad (2)$$

For the double Fourier transform, in case we assume strong scaling. That is, existence of single length and time scales, consequently a single dynamical exponent z .

$$S(k; \omega) \sim \omega^{1-\beta} k^{-(1-\alpha)} \frac{1}{k^z} \quad \text{for } k, \omega \neq 0$$

which gives,

$$S(k; \omega = 0) \sim k^{-(1-\alpha-z)} \quad \text{for } k \neq 0$$

and

$$S(k = 0; \omega) \sim \omega^{-(1-\beta-1+z)} \quad \text{for } \omega \neq 0 \quad (3)$$

It is important to examine the single Fourier transforms in equations (2). For the calculation of $S(k; \omega = 0)$ we need to take the saturated surface after a long time, but for $S(k = 0; \omega)$ we need to take the entire growing surface but locally. Thus α is related to the saturated and β to the growing surface. However, the double Fourier transform requires information of both the growing and saturated surfaces, both locally and at large length scales. Biswas et al ([10]) correctly argue that, in case there are more than one length or time scales associated with the process, the double Fourier transform should provide a much clearer picture.

2. The Statistical Model

3. The statistical model for atomic deposition

Atomic deposition has many features in common with granular deposition. The added feature is atomic binding. In the usual deposition geometry, a randomly fluctuating flux of atoms is incident on a substrate. Atoms deposit on the surface of the substrate and diffuse along it to minimize the energy. A cloud of unbonded atoms envelope this deposit and continuously exchange atoms with it through evaporation and re-deposition.

While non-equilibrium growth has been extensively studied by coarse-grained classical stochastic equations ([7]), it is not obvious a priori that the microscopic

energetic constraints relevant to atomic surfaces would automatically be satisfied by largely heuristic classical terms. In an earlier communication ([11]) we had presented electronic energy calculations in support of our model of surface growth.

Among various physical processes which have been taken into account in models of growing interfaces, surface diffusion has been considered as the most important process involved. One such model involves the linear fourth-order Mullins-Herring continuum equation ([12, 13]) supported by the discrete model of Wolf and Villain (WV) ([14])

$$\partial h(\underline{r};t)/\partial t = -D \nabla^4 h(\underline{r};t) + \eta(\underline{r};t) \quad (4)$$

where $h(\underline{r};t)$ is the height of the interface from some mean height $\langle h(\underline{r};t) \rangle$ and $\eta(\underline{r};t)$ represents Gaussian white noise as usual. This equation yields a large roughness exponent $\alpha = 1.5$ in $d=1$.

In an earlier communication ([11]) we had presented a model to look at the effect of desorption or evaporation on relatively immobile atoms which are bonded to the surface. A cloud of mobile atoms above the surface arise both from the impinging atomic beam and from evaporation caused by atoms knocked out of the surface by thermal or mechanical disturbances. These are described by their local density $\rho(\underline{r};t)$. We propose a new class of growth equations with an explicit coupling between the profile of "bonded" atoms represented by the local height of the surface $h(\underline{x};t)$, and "mobile" atoms on the surface represented by their local density $\rho(\underline{r};t)$. Our equations read:

$$\begin{aligned} \partial h(\underline{r};t)/\partial t &= -D_h \nabla^4 h(\underline{r};t) - T + \eta_h(\underline{r};t) \\ \partial \rho(\underline{r};t)/\partial t &= D \nabla^2 \rho(\underline{r};t) + T \end{aligned} \quad (5)$$

where the transfer term T is given by :

$$T = \nabla^2 h(\underline{r};t) \int_0^h dx \left(\nabla^2 h(\underline{r};t) \right)^{-1} \rho(\underline{r};t) - \nabla^2 h(\underline{r};t) \int_0^{\infty} dx \left(\nabla^2 h(\underline{r};t) \right)^{-1} \quad (6)$$

where $\chi(x)$ is 1 for $x > 0$ and 0 otherwise. We describe in what follows the meaning of the above terms.

- (i) The fourth-order term in the equation (5) describes surface diffusion of bonded atoms; this is the usual WV ([14]) term where D_h represents a diffusivity. In the continuum picture surface diffusion is a manifestation of the collective motion of the bonded atoms leading to a shape rearrangement in order to minimize the chemical potential. The leading to this term is the gradient of the local chemical potential, which is assumed to be proportional to the local curvature. This assumption was shown to be valid provided we invoke the Locality Principle of Heine ([15]).
- (ii) The flowing atoms are neither bonded to one another nor to atoms on the surface. The first term in equation (5) describes normal, as opposed to surface diffusion of these mobile atoms, where the corresponding current is the gradient of the density.

- (iii) The first term in the transfer term T , equation (6), describes spontaneous generation of mobile atoms on the surface through evaporation or desorption. This could be due, for example, to thermal disturbances. We have assumed that it is easier to eject atoms weakly bonded at spiky mounds on the surface. For thermal ejection, for example, θ is a measure of the substrate temperature. The Theta function ensures that it is easier to thermally eject atoms bonded on negative curvatures, i.e. on bumps or mounds on the surface. We have assumed that the rate of evaporation is proportional to the negative curvature on a mound.
- (iv) The second term in T , equation (6), represents condensation, whereby mobile atoms accumulate and accrete preferentially at points of positive curvature, i.e. at the bottom of deep grooves where atomic coordination is large and hence bonding is strong. This term is obviously also proportional to the local density of mobile atoms.
- (v) Finally the last term is a Gaussian white noise characterized by its width η

$$h_h(\underline{r};t)h_h(\underline{r}^0;t^0) = \frac{1}{\eta^2} \delta(\underline{r} - \underline{r}^0) \delta(t - t^0)$$

We assume that growth occurs on a flat substrate; this and the absence of a preferred direction leads to the absence of anisotropy in space. In this model we have ignored the effects of Schowbel barriers.

We can visualize the following sequence of processes: first, the mobile atoms diffuse (∇^2) in the cloud above the surface. This is followed by the preferential conversion of these atoms into the bonded species at points of high positive curvature ($\nabla^2 h$) on the surface such as mounds and grooves. The term $\nabla^2 h$ models the effect of evaporation, leading to a dynamical exchange, at regions of high negative curvature, between bonded and unbonded atoms. However, the action of the $\nabla^4 h$ term is to stabilize the formation of mounds and grooves, so ultimately the overwhelming effect is a competition between roughening and smoothening of the surface. Figure 1 illustrates the effect of the terms in our model.

4. Numerical and theoretical analysis

To start with we shall analyze a model in (1+1) dimension. The substrate is one-dimensional, so that the position of the overlayer on the substrate is located by a single position variable x . The coupled equations become :

$$\begin{aligned} \frac{\partial h(x;t)}{\partial t} &= D_h \frac{\partial^4 h(x;t)}{\partial x^4} - \frac{\partial^2 h(x;t)}{\partial x^2} + \theta(x;t) \frac{\partial^2 h(x;t)}{\partial x^2} + \eta(x;t) \\ \frac{\partial \theta(x;t)}{\partial t} &= D \frac{\partial^2 \theta(x;t)}{\partial x^2} + \frac{\partial^2 h(x;t)}{\partial x^2} - \theta(x;t) \frac{\partial^2 h(x;t)}{\partial x^2} \end{aligned} \quad (7)$$

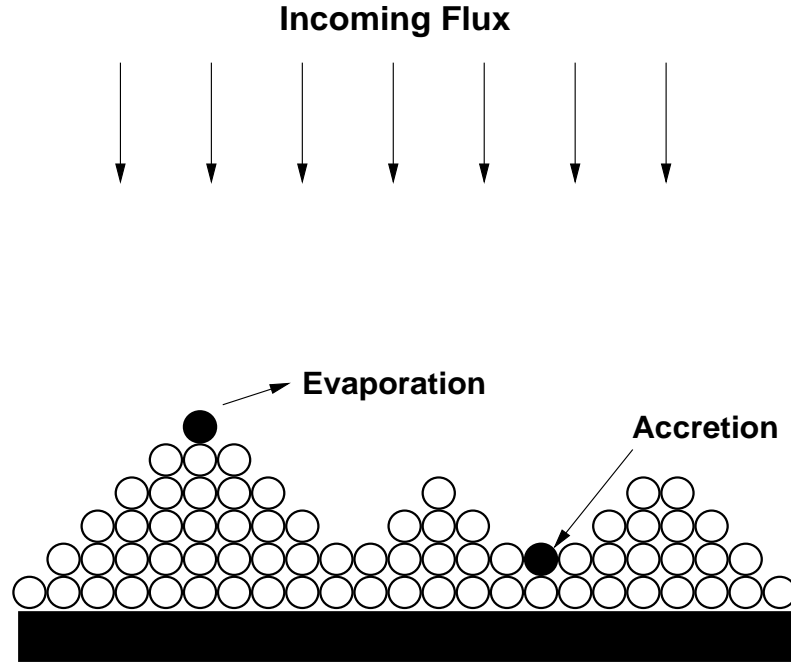


Figure 1. A pictorial depiction of the model

The Heaviside step functions in equation (6) introduces a complexity in our equations as far as analytic investigations are concerned. We shall follow the remarks of Biswas et al ([10]) and invoke a suitable representation of the Heaviside function as an infinite series. In that case, the equation (6) can be thought of as :

$$T = \frac{d^2 h(x;t)}{dx^2} + \sum_{n=1}^{\infty} \frac{d^2 h(x;t)}{dx^2} \quad (8)$$

We should note that the above expansion is not well-defined, as the coefficients of the expansion may themselves be large or divergent. As in [10], we shall still go forward in the spirit of self-consistency, i.e. subject to numerical verification. The Heaviside function introduces non-linearities. One way to gain some insight is to carry out a Hartree type mean-field approximation and replace the non-linearities by their expectation values. This leads to equations :

$$\begin{aligned} \frac{\partial h(x;t)}{\partial t} &= D_h \frac{d^4 h(x;t)}{dx^4} + \frac{d^2 h(x;t)}{dx^2} + \langle h(x;t) \rangle \frac{d^2 h(x;t)}{dx^2} + h(x;t) \\ \frac{\partial \langle h(x;t) \rangle}{\partial t} &= D \frac{d^2 \langle h(x;t) \rangle}{dx^2} + \langle \frac{d^2 h(x;t)}{dx^2} \rangle + \langle h(x;t) \rangle \frac{d^2 h(x;t)}{dx^2} \end{aligned} \quad (9)$$

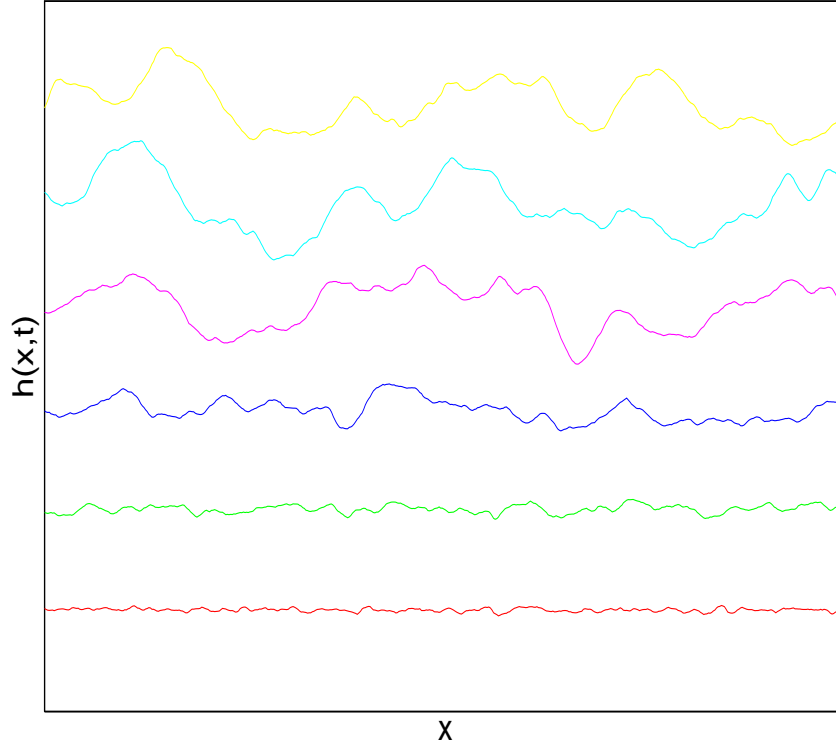


Figure 2. A part of the rough height profile at different times (bottom to top) $t = 10^3 - 10^8$ time steps. Here $D_h = D = 1$ and $\alpha = 1$, $\beta = 0.01$

where, $\hat{c} = c$ and $\hat{c} = (1 - c)$. Similar approximations have been studied by Bouchaud et al ([16]). We expect that in some regime our equations (7) will reproduce the mean field results suggested by equations (9).

Figure 2 shows a part of the growing rough height profile for $D_h = D = 1$, $\alpha = 1$ and $\beta = 0.01$. The heights have been scaled in order to bring out the detailed features for comparison. We note that with increasing time short length-scale features slowly die out and mounds and grooves spanning longer lengths are formed. Figure 3 shows the variation of the root-mean square height deviation and density as a function of time. Both quantities show saturation with time. The full dynamical description then involves both the growing and the saturated profiles.

The double Fourier transform is defined as :

$$h(k;!) = \int dx \int dt \exp[i(kx - !t)] g h(x;t)$$

The Green functions of the linear part of the equations are :

$$\frac{\tilde{h}(k;!)}{(k^0;!^0)} = G_h(k;!)(k + k^0)(! + !^0)$$

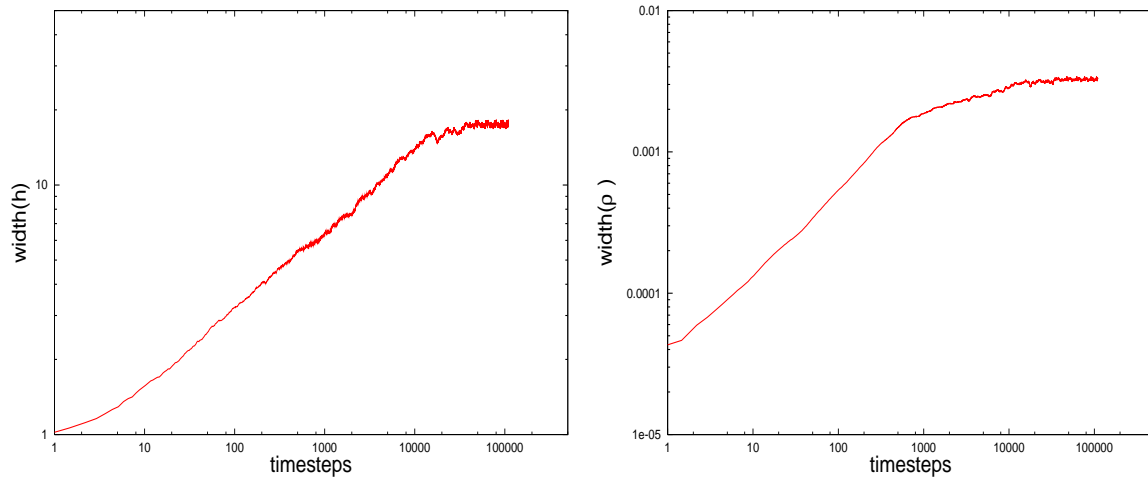


Figure 3. The height (left) and density (right) root mean square deviations as functions of time, showing saturation

$$\frac{\langle h^2(k;!) \rangle}{\langle h^2(k^0;!) \rangle} = G(k;!) (k + k^0) (l + l^0) \quad (10)$$

The correlation functions are given by :

$$\begin{aligned} S_h(k;!) &= \langle h(k;!) h(k;!) \rangle \\ S(k;!) &= \langle h(k;!) (k;!) \rangle \end{aligned} \quad (11)$$

Now from equations (7), retaining only the linear terms, we obtain the two Green functions for h and ρ ,

$$\begin{aligned} g_h(k;!) &= i! + D_h k^4 k^{2-1} \\ g(k;!) &= i! + D k^{2-1} \end{aligned} \quad (12)$$

In order to describe the scaling behaviour of the deposition process, we usually define the following scaling indices, from the correlation functions :

$$\begin{aligned} S_h(x; x^0; t; t^0) &= \langle h(x; t) h(x^0; t^0) \rangle - \langle h(x; t) \rangle \langle h(x^0; t^0) \rangle \\ S(x; x^0; t; t^0) &= \langle h(x; t) (x^0; t^0) \rangle - \langle h(x; t) \rangle \langle (x^0; t^0) \rangle \end{aligned}$$

$$\begin{aligned} S_h(x; 0) &\sim x^{2-\eta} & S(x; 0) &\sim x^2 & \text{as } x \rightarrow 1 \\ S_h(0; t) &\sim t^{2-\eta} & S(0; t) &\sim t^2 & \text{as } t \rightarrow 1 \end{aligned}$$

In general :

$$\begin{aligned} S_h(x;t) &\sim k^{-z_h} F_h(k^{-z_h} t) \\ S(x;t) &\sim k^{-z} F(k^{-z} t) \end{aligned}$$

The scaling functions $F_h(\cdot)$ and $F(\cdot)$ are assumed to be universal and the indices z_h and $z_h = z_h$; $z = z$ are the roughness and dynamical exponents. Within the strong scaling hypothesis $z_h = z$ and there exists a single time scale and a distance scale.

In the presence of two time scales, there is only a weak scaling [10] hypothesis available to us :

$$\begin{aligned} G_h(k;\omega) &= k^{-z_h} \frac{\omega^{-z_h}}{k^{z_h}}; \frac{\omega^{-z}}{k^z} \\ G(k;\omega) &= k^{-z} \frac{\omega^{-z_h}}{k^{z_h}}; \frac{\omega^{-z}}{k^z} \end{aligned}$$

Here, $z_h \neq z$. Absence of strong scaling means that the exponents z_h and z may become functions of k .

4.1. Scaling analysis for the height-height correlations

Let us look at the one loop diagram for the self-energy [10] :

$$\begin{aligned} G_h(k;\omega) &= \frac{1}{2} \int \frac{dq}{2} \frac{d\omega'}{2} G_h(k-q;\omega-\omega') k^2 (k-q)^2 S(q;\omega') \\ &\quad + \frac{1}{2} \int \frac{dq}{2} \frac{d\omega'}{2} \frac{1}{i(\omega-\omega') + (k-q)^2} \frac{1}{i\omega' + z_h(k-q;\omega-\omega')} \dots \\ &\quad \dots \frac{k^2 (k-q)^2}{q^{1+z}} \frac{(q;\omega')}{\omega' + z^2(q;\omega')} \end{aligned} \quad (13)$$

The integrand over the internal momentum q has a factor $q^{-(1+z)}$, which causes an infra-red divergence in the integral. As discussed by [10], we take care of the infra-red divergence by introducing a lower cut-off $k_0 = 1$. When we talk about "small values of momenta", we have to mean $k \ll k_0$. The argument for smaller values of k will have follow a different track.

Note also that because of the term $q^{-(1+z)}$ in the integrand, the main contribution of the integral comes from small values of q . Now, for "small" internal momenta

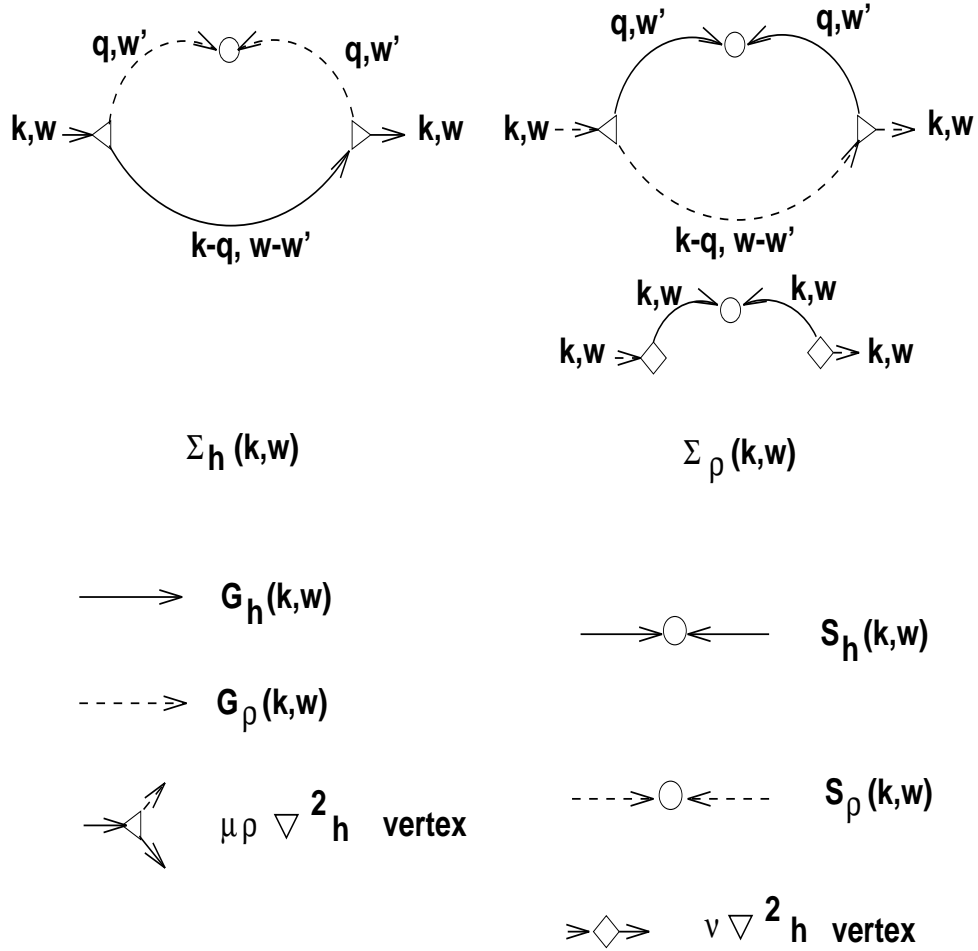


Figure 4. One loop scattering diagrams for the self-energy for the Green functions. The scattering vertices are shown at the bottom of the figure

$k = q = k_0; ! = 0 = q_h$, we can replace $G_h(k = q; ! = 0) = (i! + k^4 - k^2 + \epsilon_h(k; !))^{-1}$. We now look at $! = 0$, and noting that $(k; 0) = k^{z_h}$, we note immediately that if $z_h < 4$, then the inverse Green function is dominated by the self-energy :

$$G_h^{-1}(k; 0) = \epsilon_h(k; 0)$$

Substituting this back in the equation for the self-energy :

$$\epsilon_h(k; 0) = \frac{k^4}{(k; 0)} A \int_{k_0}^Z \frac{dq}{2} \int_{! = 0}^Z \frac{d!}{2} \frac{1}{q^{1+z}}$$

This gives :

$$\epsilon_h(k; 0) = \frac{k_0^{2-z_h}}{8} k^4$$

Since, by definition $\epsilon_h(k; 0) = k^{z_h}$, it follows immediately that $z_h = 2$

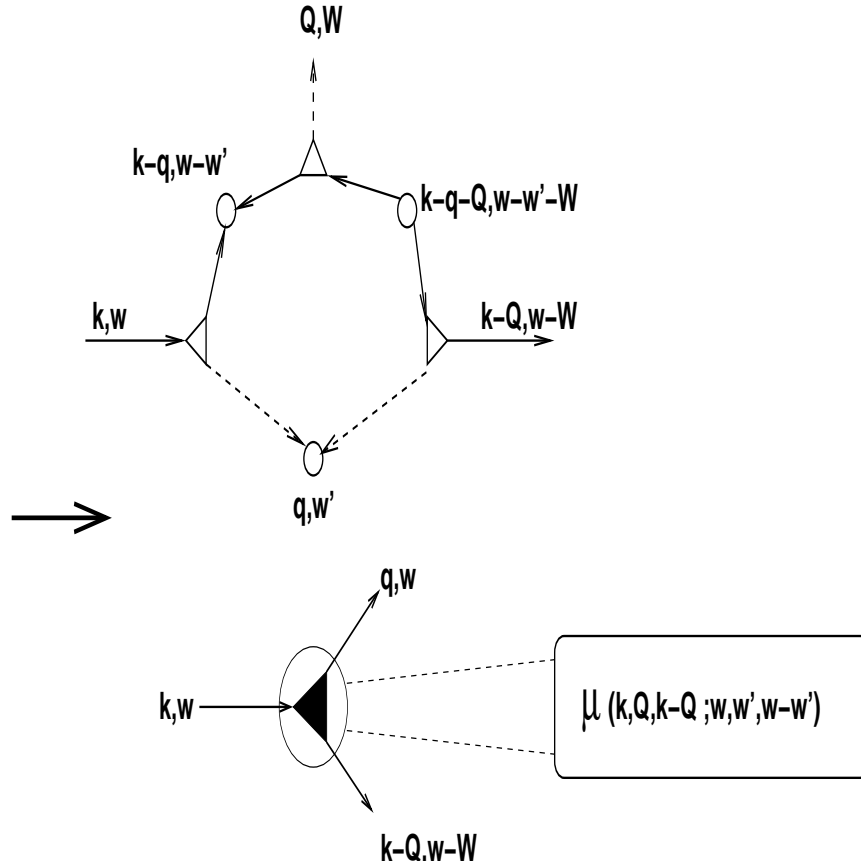


Figure 5. Vertex renormalization

Here we have considered only the bare one-loop diagram. In general, the scattering terms leads to a renormalization of the vertex through the introduction of vertex functions $\mu(k, q; k - q)$ for $q \neq 0$. The renormalization is illustrated in figure 5. For $q \neq 0$, we may assume $\mu(k, 0; k) = k^x$. Putting these back into the equation for the self-energy, we note that z_h is renormalized to $z_h + \epsilon$ where $\epsilon = x/2$. The exact numerical values for z_h may then differ from 2.

The one-loop correction to the height-height correlation function is shown in figure (6). We may immediately write :

$$S_h(k; l) = \frac{1}{l^2 + j_h(k; l)^2} \left[1 + \frac{1}{2} \frac{d}{d\epsilon} \frac{d}{d\epsilon} \left(\frac{k - q}{k} \right)^4 S_h(k - q; l - l') S(q; l') \right]$$

Let us first examine the terms on the right-hand side :

$$= \frac{1}{l^2 + j_h(k; l)^2} \left[1 + \frac{1}{2} \frac{d}{d\epsilon} \frac{d}{d\epsilon} \left(\frac{k - q}{k} \right)^4 \frac{1}{q^{1+2z_h}} \dots \right]$$

$$\dots \frac{(q; l')}{l^2 + j_h(q; l')^2} \frac{j_h(k - q; l - l')}{(l - l')^2 + j_h(k - q; l - l')^2}$$

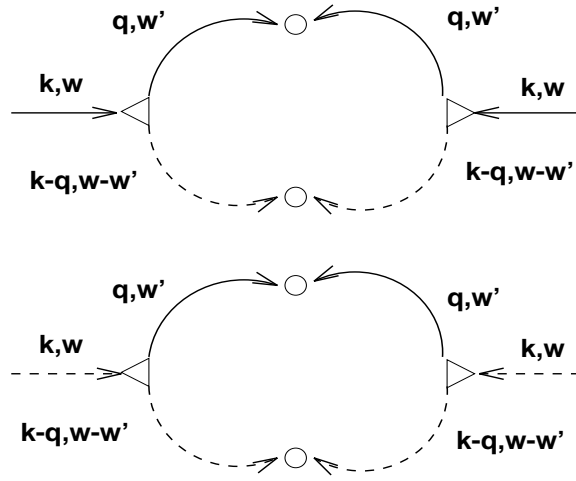


Figure 6. One-loop diagrams for the height-height and density-density correlation functions

Going back to the expression for the self-energy, we see that :

$$\Sigma_h(k; \omega) = \frac{\omega_0^2 k^4}{i\omega + \omega_0 k^2}$$

where

$$\omega_0^2 = \frac{2k_0}{8}$$

Substituting this in the expression for the correlation,

$$S_h(k; \omega) = \frac{1}{\omega^2 + \frac{\omega_0^4 k^8}{\omega^2 + \omega_0^2 k^4}} \frac{1}{1 + \frac{\omega_0 k^2}{\omega^2 + \omega_0^2 k^4}} \quad (14)$$

This is our main result from which various limits may be obtained. For instance, putting $\omega = 0$:

$$S_h(k; \omega = 0) = \frac{1}{\omega_0^2 k^4} \frac{1}{1 + \frac{1}{\omega_0 k^2}} \quad \text{for small } k$$

The numerical results are shown in figure 7. The best fit slope was found to be 6.75. Now, using the expression

$$S_h(k; \omega = 0) \sim k^{-(1+2z_h+z_h)}$$

we obtain an equation :

$$1 + 2z_h + z_h = 6.75 \quad (15)$$

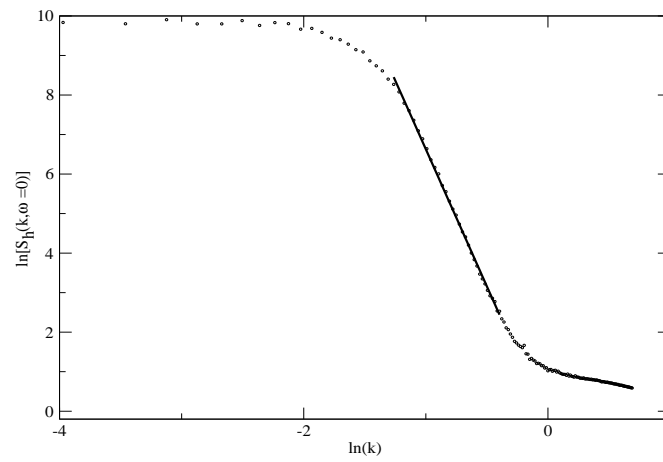


Figure 7. The Log-log plot of the double Fourier transformation $S_h(k; \omega = 0)$ vs k . For small k the slope is $1 - 2 - z_h = -6.75$

Again, putting $k=0$ and referring to figure 8 we get :

$$S_h(0; \omega) \sim \omega^{-2}$$

Numerically this has been found to be 1.996. Using the expression,

$$S_h(k=0; \omega) \sim \omega^{-(1+2-z_h+1=z_h)}$$

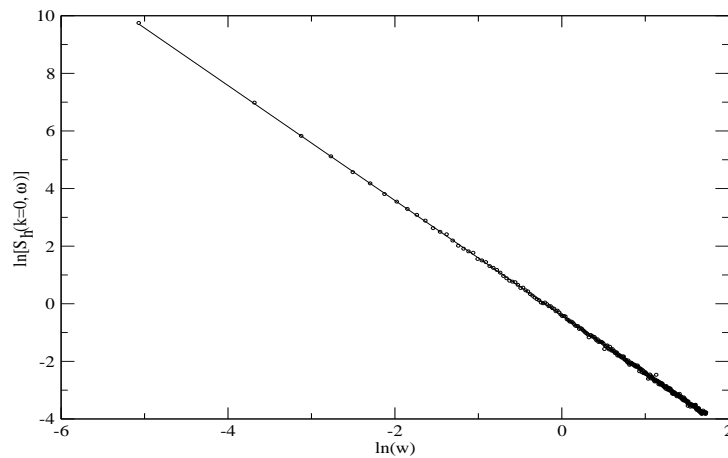


Figure 8. The Log-log plot of the double Fourier transformation $S_h(k = 0; \omega)$ vs ω . For small ω the slope is $1 - 2 - z_h = -1.996$

we get another equation,

$$1 + 2 z_h + 1 = z_h = 1.996 \quad (16)$$

Using the equations (15) and (16) and $z_h = \frac{1}{h} = \frac{1}{h}$ we estimate :

$$h = 1.2 \quad \frac{1}{h} = 0.36 \quad \text{and} \quad z_h = 3.38 \quad (17)$$

Note that numerical estimate of z_h is greater than the one-loop estimate of 2. As discussed earlier, the one-loop estimate is perturbative and may be considerably modified by vertex renormalization, as well as higher order diagrams.

We get further information from the full double Fourier transform. For example, for sufficiently small k , but $\omega \neq 0$ we get,

$$S_h(k; \omega) = A(\omega) + B(\omega) k^2$$

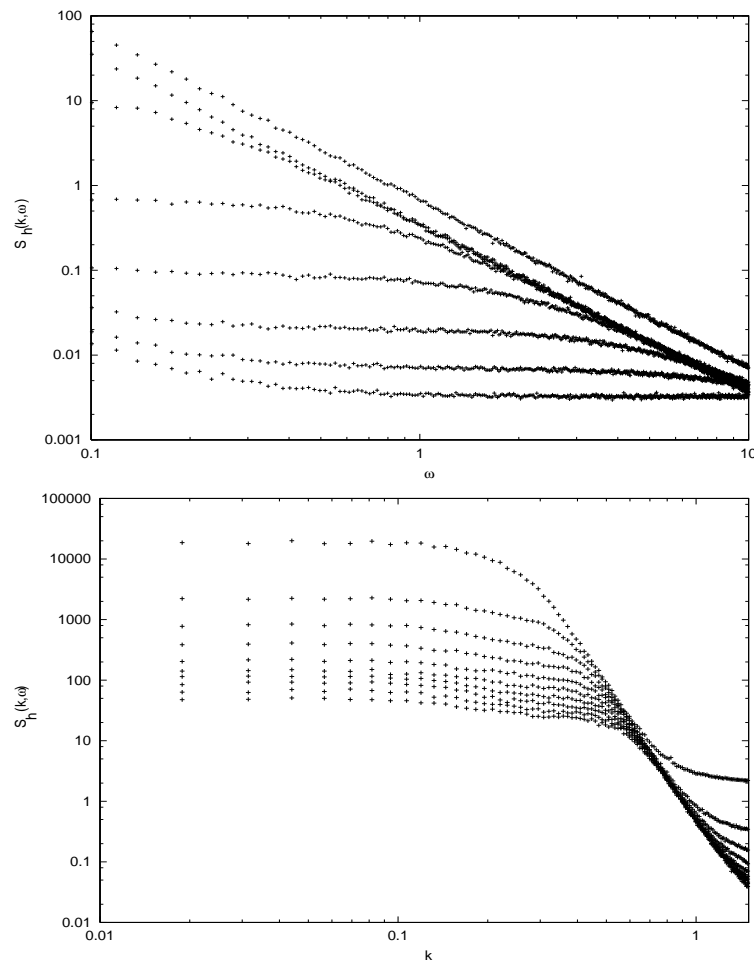


Figure 9. The Log-log plot of the double Fourier transformation $S_h(k; \omega)$ vs (top) ω for different values of k and (bottom) vs k for different values of ω .

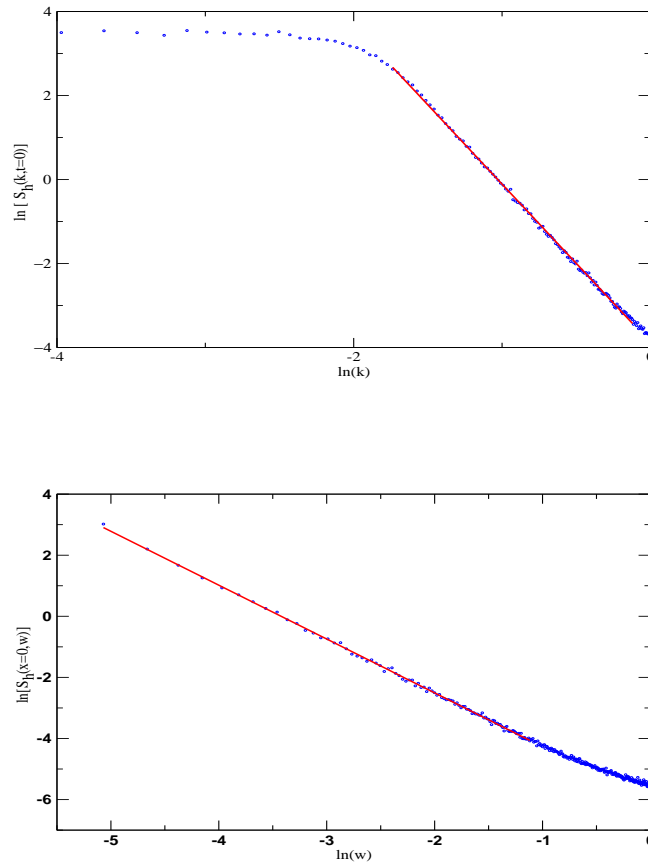


Figure 10. The Log-log plot of the single Fourier transformation (top) $S_h(k; t=0)$ vs k , fitted to the slope -1.746 and (bottom) $S_h(k=0; l)$ vs l fitted to the slope -1.763 .

As $k \rightarrow 0$ this leads to a flattening of the curve to a l -dependent constant $A(l)$. The value of k at which the flattening occurs goes on decreasing as l decreases. Similarly, for $k \neq 0$, for sufficiently small l :

$$S_h(k; l) = C(k) + D(k) l^2$$

As before, the value of l at which the flattening occurs decreases as we decrease k . This crossover behaviour is seen in our numerical results. It is easy to observe that we would not have gleaned this information from single Fourier transforms, a point emphasized earlier in the work of Biswas et al ([10]). We may interpret this as a long-time, smoothing of the growing surface and is a characteristic of the evaporation-accretion process.

In the range of k prior to flattening, we may derive:

$$S_h(k; t=0) = \frac{1}{2} \frac{d!}{d^2} S_h(k; !) + \frac{1}{2} k^{3-2z_h+z_h} \frac{d!}{(d^2 + k^{2z_h})^2} \\ A k^{z_h} + B k^{3-2z_h-2z_h}$$

Estimates of z_h and β_h are 1.37 and 0.38 respectively, consequently $z_h = 3.61$. Note that there is no reason why the estimates from single Fourier transforms and the double Fourier transform should agree exactly. For the single Fourier transforms we need information only about the saturated surface for $S_h(k; t=0)$ and the growing surface for $S_h(x=0; !)$. For the double Fourier transform, we need information for both the saturated and growing surfaces for the same function. In case there are multiple length scales in the problem that information will be reflected in the double Fourier transform [10].

From figure 10 in the $k \ll k_0$ region, attenuing suggests that :

$$S_h(k; t=0) \sim \text{const} \cdot k^{\beta_h}$$

Since $S_h(k; t=0) \sim k^{(1+2z_h)}$, the numerical results suggest that in this regime $\beta_h = 0.5$ and $z_h = 0$. In this regime, we have $S_h(k; ! = 0) \sim k^{(1+2z_h+z_h)} \sim k^0$. This crossover to a attenued regime for very small k is also seen in the numerical results of figure 7.

4.2. Scaling relations for density-density correlations

Again referring back to figure (4), we can write an expression for the self-energy for the density Green function :

$$\begin{aligned} G(k; !) &= \frac{1}{2} \frac{dq}{d^2} \frac{d!^0}{2} G(k-q; !) S_h(q; !^0) k^2 (k^2 + q^2 + k^4 S_h(k; !)) \\ &= \frac{1}{2} \frac{dq}{d^2} \frac{d!^0}{2} \frac{1}{i(d^2 - !) + (k-q; !^0)} \frac{1}{q^{1+z_h}} \dots \\ &\dots \frac{1}{d^2 + j_h(q; !^0)^2} k^2 (k^2 + q^2 + k^4 S_h(k; !)) \end{aligned}$$

We may now carry out the integral over $!^0$ and use the fact that the integrand over q has a factor $q^{(1+z_h)}$ which ensures that only small q values contribute to the integral. This, combined with a lower cut-off for q, k_0 allows us to evaluate the q integral approximately. The procedure is almost exactly like the case of height-height correlations :

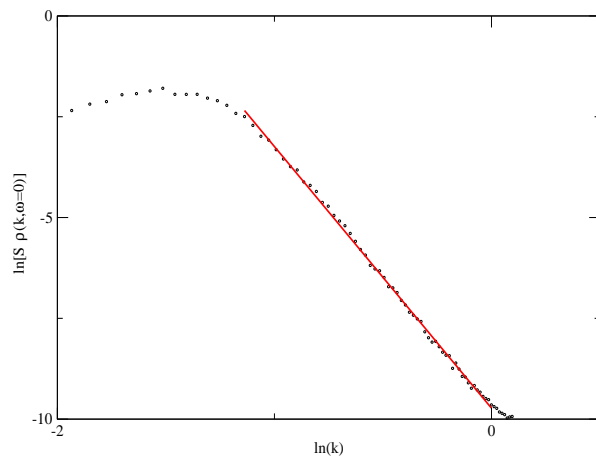


Figure 11. Log-log plot of the double Fourier transform $S(k; ! = 0)$ vs k . The best fit slope is: $1/2 - z_h = \{6.49\}$.

$$(k; ! = 0)' = \frac{\frac{1}{2}k^4}{\frac{1}{2} + \frac{1}{2}k^2}$$

For small k , we know that $(k; ! = 0) \propto k^z$, and from above equation :

$$(k; ! = 0)' = A k^2 + B k^{3/2 - z_h - z_h}$$

With $z_h = 1.5$ and $z_h = 2$, we obtain $z = 2$

For the density-density correlation function we get (again from figure (6)) :

$$S(k; ! = 0) = \frac{1}{\frac{1}{2} + \frac{1}{2}(k; ! = 0)^2} \left[1 + \int_0^z \frac{dq}{2} \frac{d!^0}{2} S_h(k - q; ! = 0) S(q; ! = 0) \right] + \frac{\frac{1}{2}k^4}{\frac{1}{2} + \frac{1}{2}k^2} S_h(k; ! = 0)$$

The first integral over q has a integrand with a factor $q^{(1+)}$, which makes sure that the main contribution to the integral comes only from small values of q . So in the integrand, we can replace $k - q$ by q and carry out the $!^0$ integral, to obtain :

$$S(k; ! = 0)' = A \left[\frac{1}{2} + \frac{\frac{1}{2}k^8}{\frac{1}{2} + \frac{1}{2}k^4} \right]^{1/2} \left[1 + \frac{0k^2}{\frac{1}{2} + \frac{1}{2}k^4} \right] \quad (18)$$

Given $z_h = 2$, $z = 2$ and $z_h = 1.5$.

$$S(k; ! = 0) \propto k^6$$

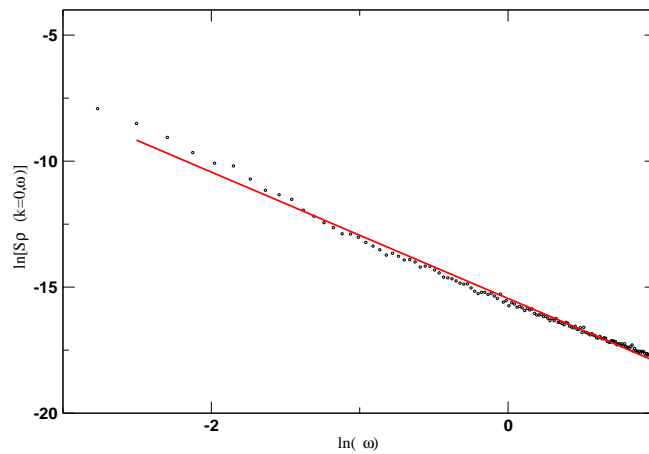


Figure 12. Log-log plot of the double Fourier transform $S(k=0;!)$ vs $!$. The best fit slope is: $1/2 \ln z = -2.48$.

From figure 11, numerically we get an index of 6.49.

In the cross-over regime when $z_h = 0$, $h = 0.5$ and $z = 2$:

$$S(k;! = 0) = \frac{k^{(3/2 - h + z_h)}}{k^{(2z_h + 2z)}} k^0$$

This is seen numerically as a flattening in the very low k regime in figure 11.

Again, integrating over the variable $!$ we get :

$$\begin{aligned} S(k;t=0) &= \int_0^Z \frac{d!}{2} S(k;!) \\ &= \left(\frac{2}{0=2} \right) \frac{1}{k^z (k^{z_h} + k^z)} \\ &= k^{-4} \end{aligned}$$

Numerically we find the index to be 3.868.

From the expression for $S(k;!)$ we note that :

$$S(k=0;!) = w^{-2}$$

Numerically we obtain an index of 2.488. We may also carry out the integral over k to get :

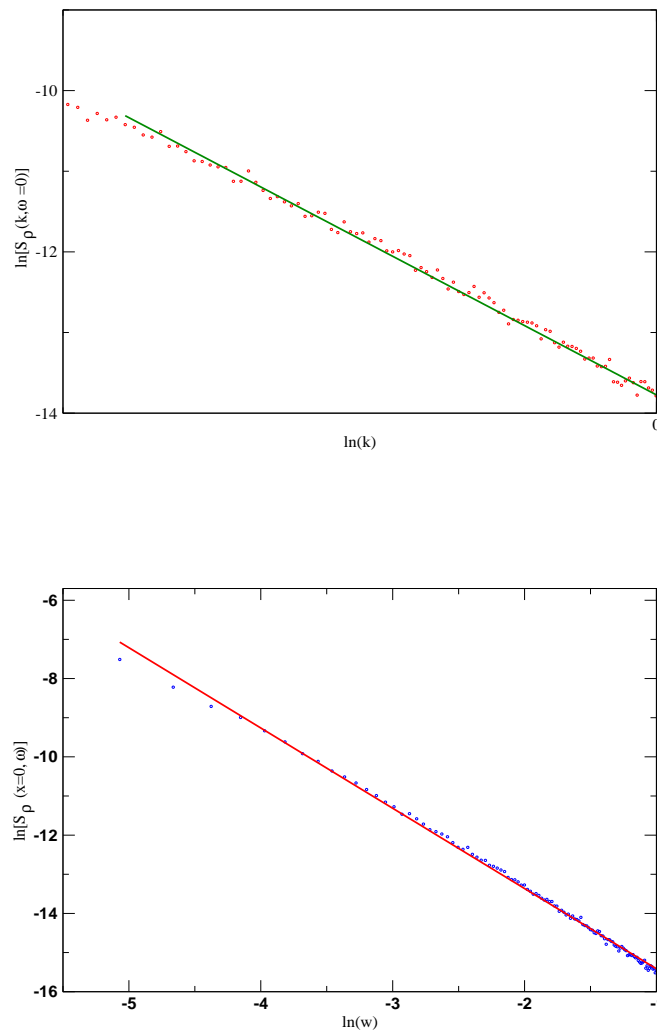


Figure 13. Log-log plot of the single Fourier transform (top) $S(k; t=0)$ vs k . The best fit slope is -3.868 (bottom) $S(x=0; !)$ vs $!$. The best fit slope is -2.050

$$S(x=0; !) = \frac{k^z}{A + B !^2} S(k; !)$$

The numerical prediction for the index is 2.05. The accompanying table summarizes our results.

Expression	Analytical Index (Single Loop)	Numerical Index	Expression	Analytical Index (Single Loop)	Numerical Index
$h(k; t=0) \text{ vs } k$	2.00	3.74	$h(k; t=0) \text{ vs } k$	2.00	2.87
$S_h(k; t=0) \text{ vs } k$	4.00	3.75	$S_h(k; t=0) \text{ vs } k$	4.00	3.89
$S_h(k=0; t) \text{ vs } t$	2.00	1.996	$S_h(k=0; t) \text{ vs } t$	2.00	2.48
$S_h(k; t=0) \text{ vs } k$	6.00	6.65	$S_h(k; t=0) \text{ vs } k$	6.00	6.49

5. Conclusion

We have studied the scaling behaviour of a set of coupled continuum equations describing surface growth in the presence of evaporation-accretion both numerically and within a one-loop perturbative approach. We notice a crossover from a roughening regime to smoothening at very large time, large length scale regimes. The one-loop estimates gives us an insight into our numerical results. We also notice that in order to study problems with more than one length-time scales, i.e. if we have weak scaling, it is essential to study the double Fourier transforms which probe both the growing and the saturated profiles together. This is in confirmation of the ideas set forward earlier by Biswas et al ([10]).

Acknowledgments

We would like to thank Dr. Anita Mehta for introducing us to the idea of coupled continuum equations and many discussions about the model we study in this communication.

References

- [1] Bak P., Tang C. and Wiesenfeld, Phys. Rev. Lett. 59 381 (1987)
- [2] Jaeger H M. and Nagel S R., Science 255 1523 (1992)
- [3] Mehta A. and Barker G C., Rep. Prog. Phys. 57 383 (1994)
- [4] Mehta A. and Barker G C., Europhys. Lett. 27 501 (1994)
- [5] Das Samanta S. and Kotliar R., Phys. Rev. B 50 R4275 (1994)
- [6] Jaeger H M., Nagel S R. and Behringer R P., Rev. Mod. Phys. 68 1259 (1996)
- [7] Mehta A., Luck J M. and Needs R J., Phys. Rev. E 53 92 (1996)
- [8] Mehta A., Barker G C., Luck J M. and Needs R J., Physica A 224 48 (1996)
- [9] Barabasi A. L. and Stanley H. E. Fractal concepts in surface growth (Cambridge University Press) (1995)
- [10] Biswas P., Majumdar A., Mehta A. and Bhattacharjee J K., Phys. Rev. E 58 1266 (1998)
- [11] Sanyal B., Mehta A. and Mukherjee A., J. Phys.: Condens. Matter 11 4367 (1999)
- [12] Herring C. Physics of powder metallurgy edited by Kingston W E (McGraw-Hill, New York) (1951)

- [13] Mullins W. W. J. Appl. Phys. 28 333 (1959); 30 77 (1959)
- [14] Wolf D. E. and Villain J. Europhys. Lett. 13 389 (1990)
- [15] Heine V., Solid State Physics (Academic Press, U.K.) 25 (1982)
- [16] Bouchaud J.P., Cates M. E., Raviprakash J. and Edwards S.F., Phys. Rev. Lett. 74 1982 (1995)